

Geometry-Based Concept for Automatic Cut Planning and Flattening of Sheet Metal Components

Jannis Korn^{1,a*}, Clemens Acksteiner^{1,b}, Sebastian Langula^{1,c},
Christina Guilleaume^{1,d} and Alexander Brosius^{1,e}

¹Chair of Forming and Machining Technology, TUD Dresden University of Technology,
01062 Dresden, Germany

^ajannis.korn@tu-dresden.de, ^bclemens.acksteiner@tu-dresden.de,
^csebastian.langula1@tu-dresden.de, ^dchristina.guilleaume@tu-dresden.de,
^ealexander.brosius@tu-dresden.de

Keywords: Sheet Metal Forming, Flattening, Cut Planning, Tailored Blanks, Remanufacturing

Abstract. Sheet metal components with complex geometries are typically recycled by remelting. Direct remanufacturing necessitates the flattening of parts, which requires the implementation of cuts to facilitate unwinding. The exact positioning of these cuts is a complex planning task, because several influencing factors can be considered, such as material usage, ease of flattening, or minimal forming required. This study presents a geometry-based concept addressing this challenge and demonstrates its use for a test geometry. The finite element method is applied to simulate the flattening process of the resulting sections, and the results are evaluated in terms of planarity and induced plastic strain. The findings of the present work indicate a discernible dependency of results on the selection of the flattening directions. In particular, curved areas impact the induced plastic deformation and springback of flattened sections. This is a crucial consideration when planarity is prioritised over material utilisation.

Introduction

Sheet metal forming is an integral process in today's manufacturing with global demand rising for decades. In light of increasing orientation towards and necessity for a more circular economy, current concepts of recycling and reuse of sheet metal must be reconsidered [1].

A promising approach involves the direct remanufacturing of existing sheet metal components, which we refer to hereinafter as "first life" components (1st LCs), with forming processes avoiding a transition through the liquid phase [2]. Despite the novelty of this research domain, pioneering studies have been conducted to assess its feasibility. In [3], the authors demonstrated the extraction of several deep-drawing blanks from a used car bonnet. Another study has considered the effects of flattening on the production of recycled parts from 1st LCs, such as the creation of a break disc cover from a car roof [4]. In both studies, large components with simple geometries and small curvatures were chosen. Improving both material utilisation and applicability of the concept to a wider variety of inputs demands cutting the 1st LCs before flattening. Subsequently, sections too small to be remanufactured directly can be utilised as patches for the recombination into tailored blanks. When manufacturing "2nd life" components out of those recombined blanks, however, the manufacturing processes have to be reconsidered. A feasible example is the use of macrostructured deep drawing tools to facilitate a larger process window, such as larger irregularities of the blanks [5].

It is evident from a survey of the relevant literature that a number of approaches for the unfolding of three-dimensional sheet metal geometries can be found. Flat pattern development using computer-aided methods is frequently based on geometry-based concepts, as the one presented in [6], or on the optimisation of other metrics as in [7]. However, these existing methods are oriented towards the creation of blanks to enable the forming of their initially considered components. In contrast, there has been no publication of concepts that analyse the explicit placement of cuts and the evaluation of the flattenability of the resulting sections for 1st LCs intended for direct remanufacturing, for example into second life tailored blanks.

Accordingly, this work addresses the following research question: How can a geometry-based, automated cut planning strategy be designed to generate flattenable sections from first life components for subsequent use as second life sheet metal blanks? Within this study, a concept addressing this question is presented and employed to demonstrate first results. Additionally, finite element analysis is utilised to simulate the flattening of the resulting cut sections and the outcomes are evaluated in terms of flatness and induced plastic strain. As example geometry for the demonstration of the process we choose a T-cup as shown in Fig. 1a. It offers moderate complexity and incorporates several aspects typical to deep drawing parts such as plane surfaces and features with single as well as double curvatures with a range of different radii. Further details on the geometry can be found in [8]. The process is aimed to be performed on a surface mesh derived from a 3D scan of a 1st LC serving as its digital twin. In this work, however, a manually constructed mesh is used to reduce artefacts.

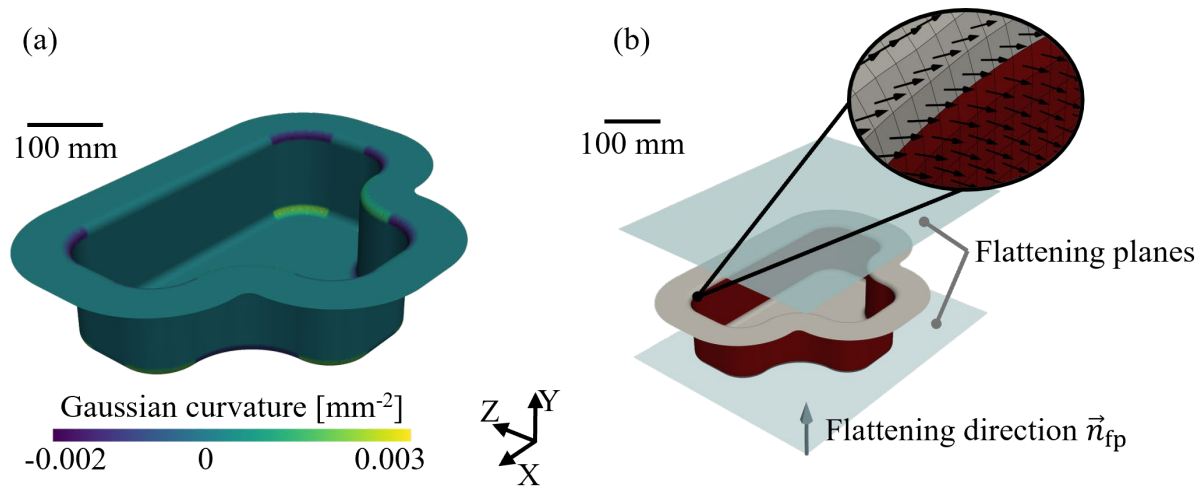


Fig. 1. (a) Isometric view of the T-cup and visualisation of Gaussian curvature. (b) Critical zones for flattening with the flattening planes shown. The determination is based on the angle of the face normals in relation to the direction of flattening.

Methods and Simulation Procedure

The methodology proposed in this paper as a first concept towards an automatic placement of the required cuts is motivated by the observation that areas orthogonal to the flattening plane can lead to instability and buckling during the flattening process. Consequently, this study suggests a semi-automatic algorithm to remove these areas of conflict subsequently. The individual modules of the process are shown in Fig. 2.

The discrete surface mesh of a 1st LC is considered the input for the subsequent algorithm. When applied to a digital twin, this can be obtained from a 3D scan of the geometry and subsequent mesh generation from the obtained data. For the purpose of this work, a mesh with quadrilateral shell elements was considered, obtained from a component designed using CAD. The coordinate system is aligned with the prominent features and symmetries of the T-cup. In the subsequent modules, the preparation and cutting of the mesh are performed in Python using a combination of self-written algorithms and mesh operations using the package PyVista [9].

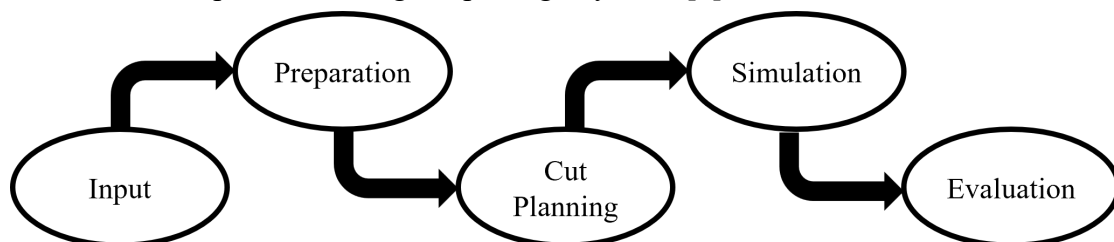


Fig. 2. Schematic overview of the process.

Preparation. In preparation for the cut planning, the Gaussian curvature is initially computed to remove regions with nonzero values beyond a predefined tolerance range. This helps reduce the problem's complexity as areas with nonzero curvatures are generally considered non-developable without additional information [10]. The tolerance range is identified by means of manual inspection, thus ensuring that only areas exhibiting double curvature are removed. For the test geometry used in this study, this range was set to $[-10^{-4} \text{ mm}^{-2}, 10^{-4} \text{ mm}^{-2}]$ to remove the visibly distinctive regions of double curvature seen in Fig. (1a).

In order to circumvent any modification of the residual geometry, the removal is executed by identifying the boundaries of the designated areas. The thus obtained nodes are duplicated. Adjacent faces are sorted according to their relative position to the edges. Finally, the faces to one side of the boundary are redefined to use the duplicated instead of the original nodes. By identifying unconnected regions of the mesh, the parts are then separated.

The remaining test geometry is remeshed before the application of the subsequent algorithms. This ensures a regular and smooth mesh, thereby reducing artefacts.

Cut Planning. The thus prepared mesh is then used as an input to the proposed algorithm for placing the cuts. Initially, a flattening plane is defined via the flattening direction, i.e. its normal vector \vec{n}_{fp} , as shown in Fig. 1b. After manually setting a tolerance angle θ_{tol} , the angles φ_i between \vec{n}_{fp} and all face normals \vec{n}_i are calculated. For the study of our test geometry, a value of 10° was selected as it ensured the exclusion of artefacts. The outer boundary of sections with angles of $90^\circ \pm \theta_{tol}$ is determined as cutting paths. Finally, the mesh is separated along those lines in the same way the doubly curved areas were removed. Sections with angles outside the defined interval are considered flattenable within the plane defined by \vec{n}_{fp} while the removed sections can be reconsidered with a different flattening plane to improve material utilisation.

To prepare the obtained sections for the subsequent finite element analysis, they are semi-automatically placed. This process is initiated by subjecting them to a gravitational simulation above an impenetrable plane. Fully automating the procedure requires more research on how to properly account for various challenges such as metastable positions.

Simulation of the Flattening Process. To analyse the flattening behaviour, finite element simulations are carried out using LS-DYNA (R15.0.2) with implicit time integration. The simulation model is visualised in Fig. 3a. It comprises two rigid plane dies with the parts to be flattened placed in between them. All parts are meshed with fully integrated quadrilateral shell elements (ELFORM -16) with 7 through thickness integration points and 1 mm element edge size.

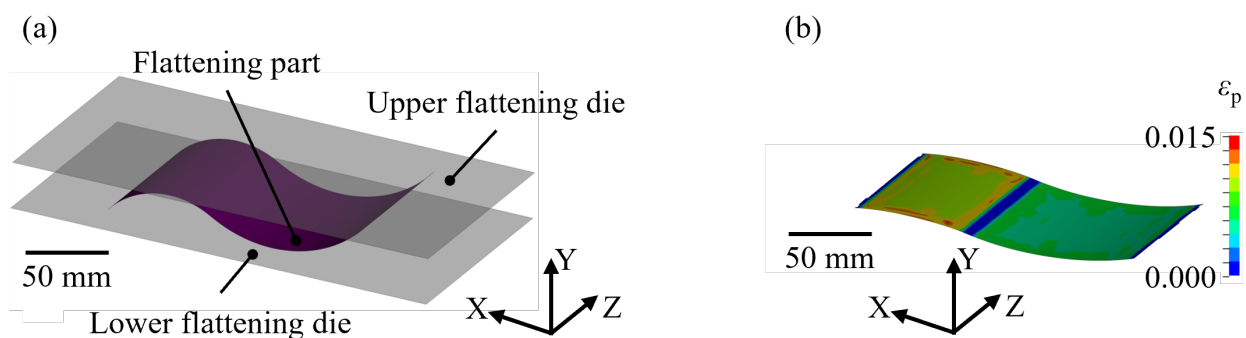


Fig. 3. (a) Simulation model and (b) plastic strain after springback.

With regard to material modelling, the sections consist of DP600 steel assuming isotropic properties. This dual phase steel is characterised by good formability and is commonly used in the automotive sector. The blank thickness and the parameters for modelling the dual phase steel are taken from [11]. They are listed in Table 1. Note that flow stress σ_f is given as a function of effective plastic strain ϵ_p .

During the flattening process the dies are closed via position control of the upper die (*BOUNDARY_PRESCRIBED_MOTION_RIGID) until their distance equals the initial blank

thickness of 1.16 mm. In the course of this, a Coulomb friction model is applied with a friction coefficient of 0.1. After flattening, a static springback simulation is performed (Fig. 3b).

Table 1. Parameters for modelling DP600 [11].

Parameter	Value
Flow stress σ_f [MPa]	$1060 (0.001 + \varepsilon_p)^{0.174}$
Young's modulus [GPa]	185
Poisson's ratio [-]	0.3
Sheet thickness [mm]	1.16

Evaluation of the Flattened Parts. Following flattening, the planarity has to be analysed. In this work, this is done by assessing the distances of the finite nodes to a best fit plane. From literature it is known that one can use principal component analysis (PCA) with the aid of singular value decomposition (SVD) to calculate a best fitting plane [12]. Thus, the plane is described via the centroid of the point data and the third principal component as the normal vector of the plane. Thereafter, the distances to the obtained plane and in particular their extrema in positive and negative direction are computed (Fig. 4).

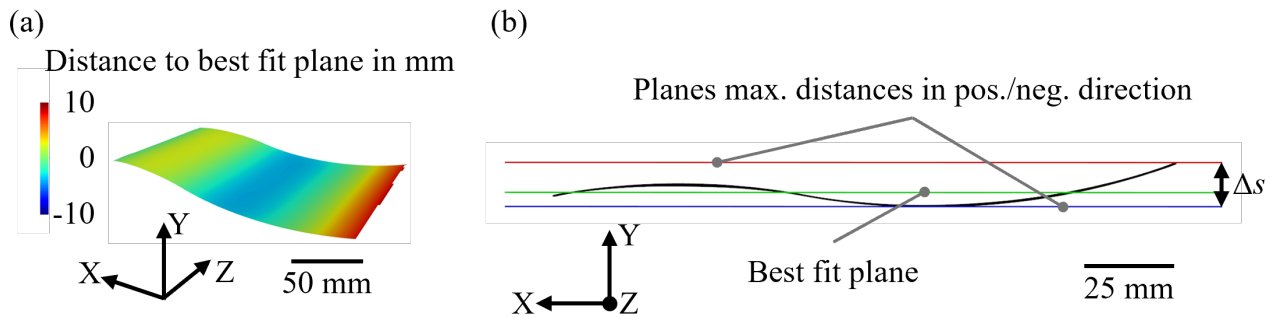


Fig. 4. (a) Distances to best fit plane. (b) Planes of maximum distances in positive and negative direction to the best fit plane.

Results

Cut Planning. In order to find a discrete approach for choosing the flattening plane normal, the scope of this study was limited to the planes defined by the standard base vectors of the chosen coordinate system. This leads to 6 different permutations for the sequential application of the algorithm. Here, only two applications were considered as it does not reduce the number of studied cases. To indicate the nature of their creation, cut sequences are identified based on the normals of the flattening plane used, i.e. “cut parts XY” are generated by considering flattening directions in x and y direction subsequently.

Table 2. Quantitative results of cut planning.

Sequence of flattening directions	Number of resulting sections	Degree of material utilisation [%]
XY	10	90.4
XZ	8	49.3
YX	10	90.4
YZ	10	90.4
ZX	8	60.8
ZY	10	90.4

Of the 6 examined cut results, combinations of the same flattening directions with different permutations lead to almost identical sections. The number of resulting sections after consideration of two flattening planes is compiled in Table 2 together with the degree of material utilisation. To

assess the latter quantity, the surface area of all flattenable sections was divided by the total area of the initial mesh before preparation without taking into consideration the quality of the flattened sections. A more informed assessment of effective material utilisation requires additional research on the requirements of the recombination step mentioned in the introduction of this work. The flatness of components, both in terms of local edges and global geometry, is likely to act as a limiting factor to the areas considered usable. Depending on the process design and the geometry of the 1st LC, it will furthermore be important to consider the impact of existing and induced plastic strains, the result of which may be additional limitations. While these factors may result in the evaluation of certain sections as unusable and subsequently in the development of more complex strategies for the cut planning, they represent areas that require further investigation and therefore did not form the primary focus of the present work.

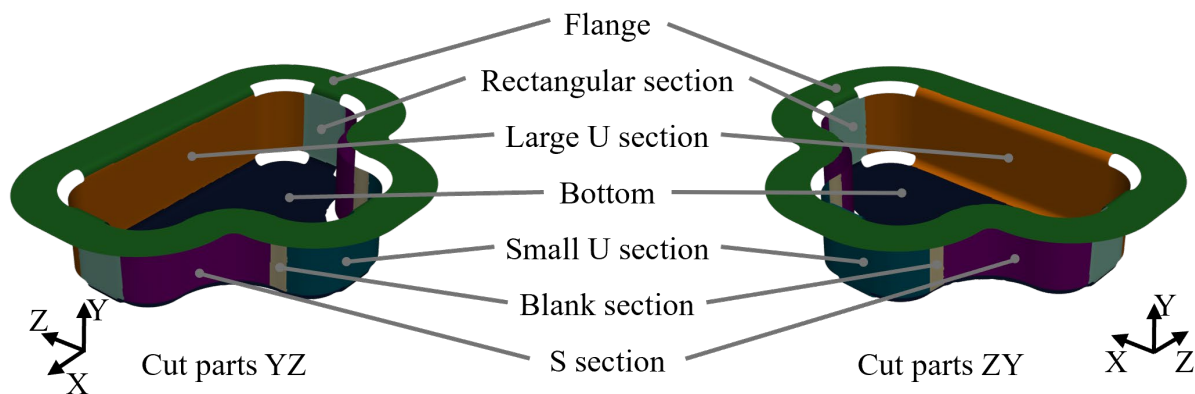


Fig. 5. Overview and definition of nomenclature for resulting cut sections after algorithm application for flattening plane normal in y- and z-direction with different orders of application.

Sections with similar geometries are coloured identically for better visual distinction.

The outcomes derived from analogous flattening directions in disparate permutations primarily diverge in the allocation of the singly curved areas between the sidewall and the flange, or the bottom, of the T-cup. This phenomenon can be observed for the four combinations with equal degree of material utilisation, an illustrative example is provided by the large U section in Fig. 5. The remaining two combinations, XZ and ZX, do not consider flattening in the direction of the original drawing process. Therefore, a third iteration of the algorithm would be necessary to improve their material utilisation, as there remain unflattenable sections after the initial two.

Depending on the missing flattening direction, it is evident that the cut sections exhibit distinct geometries, which can only be accurately compared in pairs. Consequently, the ensuing analysis will concentrate exclusively on the sections derived from the YZ and ZY cuts. Of the combinations examined, these provide the broadest spectrum of geometrical features and, consequently, a better insight into effects on flattenability. A descriptive nomenclature for the different sections is chosen, its details are shown in Fig. 5. Symmetrical parts were only simulated once per cut permutation while the band sections were omitted completely due to their small size and pre-existing planarity.

Flattening. After cutting, the resulting sections are flattened via the presented simulation process. In Fig. 6, the differences of the minimum and maximum signed distances Δs as well as the standard deviation $\sigma(s)$ of distances to the best fit plane are visualised for each considered section and cutting sequence. Sections comprising the most proportion of initially flat area, namely flange, bottom and rectangular section, have the smallest differences Δs and standard deviations $\sigma(s)$. The values are declining in the aforementioned order. Bottom and flange of cut parts ZY have higher planarity compared with their counterparts. This is due to cut parts YZ producing more contiguous radii for these sections.

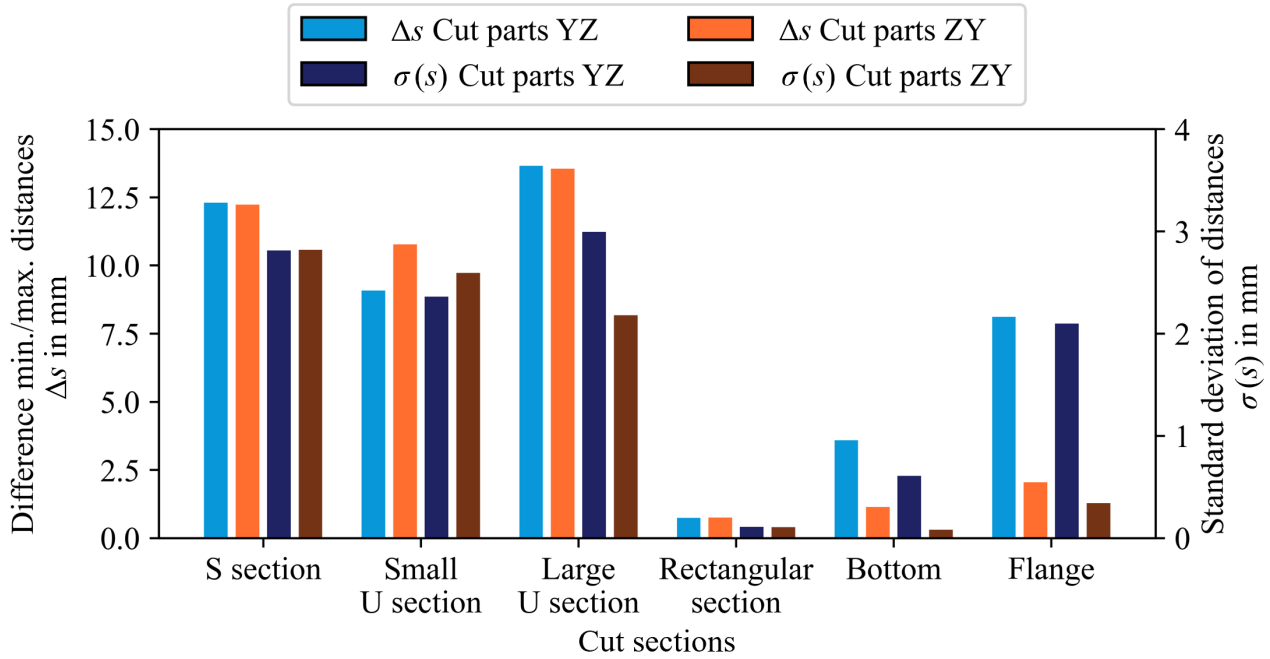


Fig.6. Distances to best fit plane after flattening.

Fig. 7 exhibits the distribution of effective plastic strains in a violin plot. Two local maxima can be seen in the distribution for each of the U sections. The one at higher strains is corresponding to the flattened area of the initially eponymous curvatures. Conversely, the second maximum can be attributed to the originally flat area. For the large U sections, a major proportion of these parts is experiencing a negligible amount of plastic strain. In contrast, almost the whole small U sections are plastically deformed. Cut parts ZY leads to higher plastic strains for the U sections as the contiguous radii account for a larger proportion of those parts. These radii are resulting in lower planarity for the small U section, while for the large one the difference Δs is almost the same (Fig. 6).

Finally, the nearly identical S section cuts result in similar planarity and plastic strain distributions. The two peaks in the violin plot in Fig. 7 indicate the two main radii of those sections. Here, the smaller radius and the associated smaller area cause higher strains but a reduced contribution to the overall distribution.

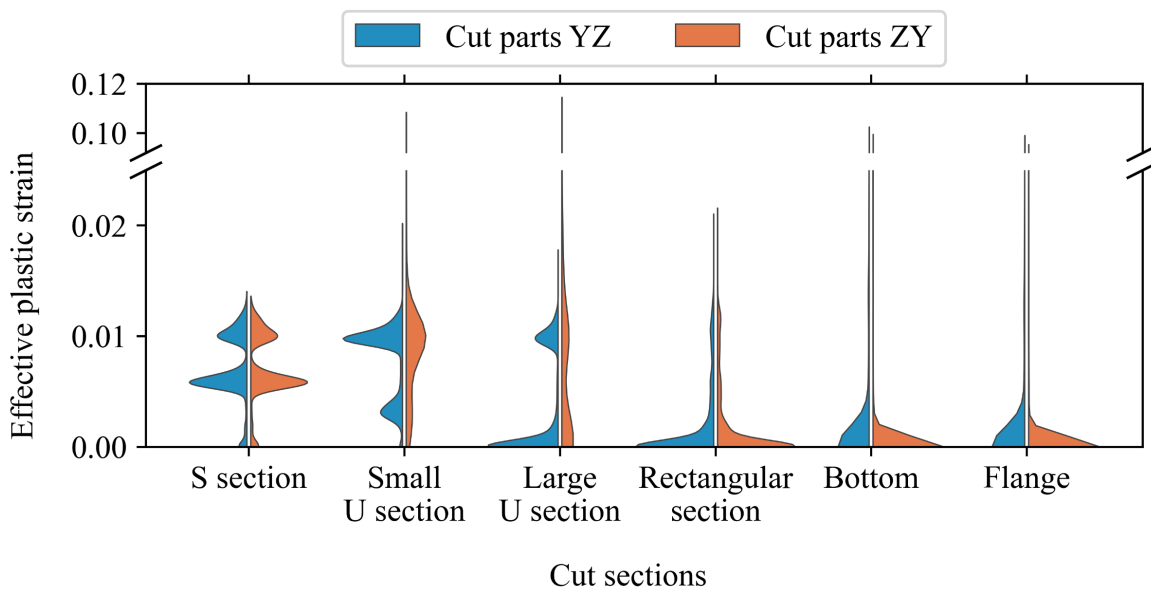


Fig. 7. Distribution of effective plastic strain after flattening.

An exemplary display of the spatial deviations from planarity is shown in Fig. 8 for the flange and small U section because for those sections the influence of the previously mentioned contiguous radii

is clearly visible. For the flange, an overall bending with uplifting sides can be observed for cut parts YZ. In comparison, the more pronounced curvatures for the small U section of cut parts ZY provokes tilting of the flattened specimen around the x-axis.

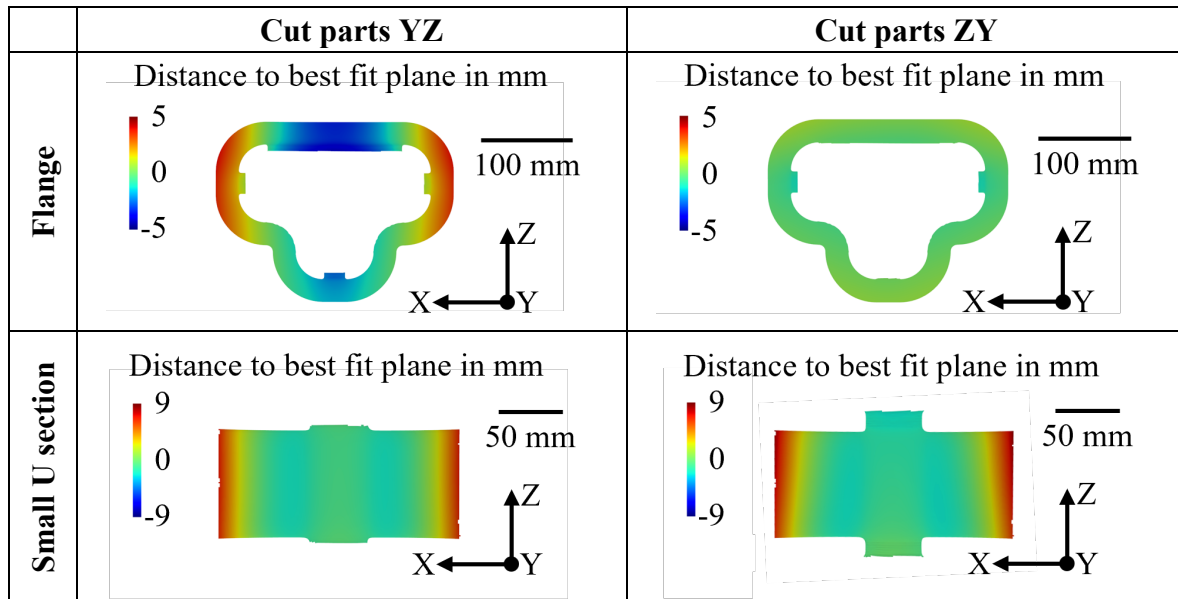


Fig. 8. Height profiles after flattening.

Conclusion and Outlook

This study proposes an approach to the flattening of sheet metal components by means of inducing cuts along regions orthogonal to the flattening plane and demonstrates the procedure on the example geometry of a T-cup. By analysing the resulting sections using a finite element simulation, it was shown that the choice of flattening directions is not only pivotal for the number of cuts required but also influences the flattenability of the resulting sections. Both induced amount of plastic strain and springback are influenced by radii in the geometry. While regions with large curvature had a distinctive influence on sections with overall small to no curvature, their effects on more curved geometries were less pronounced. This emphasises the significance of curved areas for the flattenability of 1st LCs and underscores the necessity for further investigation.

Our findings indicate that the proposed concept has the potential to serve as a viable building block for the direct recycling of 1st LCs. However, it is crucial to note that further investigation into alternative geometries is necessary to ensure the applicability of this method. It is evident that the approach for the cut placement is geometry-based; consequently, mechanical properties have not been considered, despite their obvious influence on the problem. Moreover, it is imperative that the robustness and automation of the process be further developed prior to its realistic application to digital twins.

Acknowledgements

This work was supported by the Werner Siemens Foundation under the project “Second Life Metal Components – A Pathfinding Project for Upcycling”.

The authors gratefully acknowledge the computing time made available to them on the high-performance computer at the NHR Centre of TU Dresden. This centre is jointly supported by the Federal Ministry of Research, Technology and Space of Germany and the state governments participating in the NHR (www.nhr-verein.de/unsere-partner).

References

- [1] J. M. Allwood, M. F. Ashby, T. G. Gutowski, and E. Worrell, ‘Material efficiency: A white paper’, *Resources, Conservation and Recycling*, vol. 55, no. 3, pp. 362–381, Jan. 2011, doi: 10.1016/j.resconrec.2010.11.002.
- [2] J. M. Allwood, J. M. Cullen, and R. L. Milford, ‘Options for Achieving a 50% Cut in Industrial Carbon Emissions by 2050’, *Environ. Sci. Technol.*, vol. 44, no. 6, pp. 1888–1894, Feb. 2010, doi: 10.1021/es902909k.
- [3] J. A. Österreicher, F. Grabner, P. Oberhauser, S. L. Hovden, and C. M. Schlögl, ‘Toward a Circular Economy in Deep Drawing: Remanufacturing End-of-Life Automotive Parts’, *MATEC Web Conf.*, vol. 408, p. 02026, 2025, doi: 10.1051/mateconf/202540802026.
- [4] R. Haase, D. Farioli, R. Selbmann, M. Werner, and V. Kräusel, ‘Dismantling and remanufacturing strategies in the automotive sector’, *Procedia CIRP*, vol. 122, pp. 695–700, 2024, doi: 10.1016/j.procir.2024.01.096.
- [5] A. Mousavi, “A novel approach towards a lubricant-free deep drawing process via macro-structured tools,” Ph.D. dissertation, Chair of Forming and Machining Technology, TU Dresden, Dresden, Germany, 2019.
- [6] X. Liu, S. Li, X. Zheng, and M. Lin, ‘Development of a flattening system for sheet metal with free-form surface’, *Advances in Mechanical Engineering*, vol. 8, no. 2, Feb. 2016, doi: 10.1177/1687814016630517.
- [7] Q. Liu, J. Xi, and Z. Wu, ‘An energy-based surface flattening method for flat pattern development of sheet metal components’, *Int J Adv Manuf Technol*, vol. 68, no. 5–8, pp. 1155–1166, Apr. 2013, doi: 10.1007/s00170-013-4908-y.
- [8] A. Wolf et al., ‘Modeling metal forming of a magnesium alloy using an adapted material model’, *Engineering Reports*, vol. 4, no. 7–8, June 2022, doi: 10.1002/eng2.12540.
- [9] C. Sullivan and A. Kaszynski, ‘PyVista: 3D plotting and mesh analysis through a streamlined interface for the Visualization Toolkit (VTK)’, *JOSS*, vol. 4, no. 37, p. 1450, May 2019, doi: 10.21105/joss.01450.
- [10] A. Cucakovic A., B. Jovic S., and M. Tripkovic R., ‘Paper strips driven design: Application on doubly curved surfaces’, *FME Transaction*, vol. 45, no. 2, pp. 251–255, 2017, doi: 10.5937/fmet1702251c.
- [11] N. Küsters, “Halbanalytische Methode zur Charakterisierung der Fließortkurven von Blechwerkstoffen,” Ph.D. dissertation, Chair of Forming and Machining Technology, TU Dresden, Dresden, Germany, 2020.
- [12] A. Nurunnabi, D. Belton, and G. West, ‘Diagnostics based principal component analysis for robust plane fitting in laser data’, *16th Int’l Conf. Computer and Information Technology. IEEE*, pp. 484–489, Mar. 2014. doi: 10.1109/iccitechn.2014.6997319.